





Title	Integrated dual optical frequency comb source
Authors	Alexander, Justin K.;Caro, Ludovic;Dernaika, Mohamad;Duggan, Shane P.;Yang, Hua;Chandran, Satheesh;Martin, Eamonn P.;Ruth, Albert A.;Anandarajah, Prince M.;Peters, Frank H.
Publication date	2020-05-21
Original Citation	Alexander, J. K., Caro, L., Dernaika, M., Duggan, S. P., Yang, H., Chandran, S., Martin, E. P., Ruth, A. A., Anandarajah, P. M. and Peters, F. H. (2020) 'Integrated dual optical frequency comb source', Optics Express, 28(11), pp. 16900-16906. doi: 10.1364/OE.384706
Type of publication	Article (peer-reviewed)
Link to publisher's version	http://www.opticsexpress.org/abstract.cfm?URI=oe-28-11-16900 - 10.1364/OE.384706
Rights	© 2020 Optical Society of America under the terms of the OSA Open Access Publishing Agreement - https://www.osapublishing.org/library/license_v1.cfm#VOR-OA
Download date	2024-05-14 21:12:57
Item downloaded from	https://hdl.handle.net/10468/10263

Integrated dual optical frequency comb source

JUSTIN K. ALEXANDER,¹ LUDOVIC CARO,² MOHAMAD DERNAIKA,^{2,3} SHANE P. DUGGAN,^{3,4} HUA YANG,² SATHEESH CHANDRAN,^{4,5} EAMONN P. MARTIN,⁶  ALBERT A. RUTH,^{4,5}  PRINCE M. ANANDARAJAH,⁶  AND FRANK H. PETERS^{3,4,*} 

¹*Aeponyx, Canada*

²*Rockley Photonics, Ireland*

³*Integrated Photonics Group, Tyndall National Institute, Cork, Ireland*

⁴*Dept. of Physics, University College Cork, Ireland*

⁵*Environmental Research Institute, University College Cork, Ireland*

⁶*Photonics Systems and Sensing Lab, School of Electronic Engineering, Dublin City University, Ireland*

**f.peters@ucc.ie*

Abstract: A monolithically integrated dual-channel optical frequency comb source is demonstrated in this paper. Three lasers are integrated on a single chip using a regrowth-free fabrication process in a master-slave-slave configuration. The master laser's power is split equally using a 1x2 multimode interference coupler and injection locks the two slave lasers. The slave lasers are gain-switched to produce dual optical frequency combs at 4.1 GHz and 5 GHz. To the best of our knowledge, this is the first demonstration of a dual optical frequency comb source with all light sources monolithically integrated in a photonic integrated circuit (PIC).

© 2020 Optical Society of America under the terms of the [OSA Open Access Publishing Agreement](#)

1. Introduction

Optical frequency combs (OFCs) have been shown to have applications in both telecommunications [1,2] and spectroscopy [3–6]. Recently, the use of dual OFCs has become of interest for trace-gas detection systems [3]. Generating two coherent OFCs with slightly differing repetition rates and beating them together on a photodiode produces a radio frequency (RF) spectrum of tones spaced at the difference of the OFC repetition rates. In this way, the optical domain comb is translated to the RF domain. The change in optical intensity due to absorption, as one or both of the combs is passed through a gas sample, will change the RF beat spectrum which can be used to identify the specific gas.

The method of comb generation used in this paper is based on gain-switched injection-locked lasers. Gain switching enables tunable line spacing, while injection locking leads to the gain-switched laser retaining the linewidth of the master laser, while also reducing the phase noise in the higher speed Fabry Pérot slave lasers [7]. This design choice can also be monolithically integrated [8–10]. A dual comb source using discrete components was previously demonstrated using this method [11]. The complexity of a dual comb source test set-up can be greatly reduced through photonic integration. Integrating the required components on to a single chip greatly reduces size, simplifies coupling, and can even remove polarization dependencies. An integrated dual comb source was recently achieved using micro-resonators on silicon [12], but this design requires an external laser.

The device described in this paper is a monolithically integrated dual channel optical comb source. Previous research on comb sources and integration helped inform the design of this device [7,10,13–16].

2. Device design

The device was fabricated on commercially available lasing material designed for emission at 1.55 μm with an InP substrate, purchased from the company IQE. The material consists of 5 compressively strained AlGaInAs quantum wells on an n-doped (100) InP substrate, with a total active region thickness of 0.41 μm . The upper p-doped cladding consists of a 0.2 μm InGaAs cap layer, followed by 0.05 μm of InGaAsP, lattice matched to 1.62 μm of InP. The device was designed to operate with a single lateral mode based on single mode waveguide designs.

The device consists of a master laser which couples to two slave lasers. This is achieved using a 1x2 MMI (multi-mode interference coupler) to split the power of the master laser equally between two branches. The master laser is a 2-section SFP (slotted Fabry-Pérot) with a gain section and a slotted section. The slotted section features 8 equally spaced shallow etched slots with a slot spacing of 100 μm , connected to a straight 550 μm gain section for a total length of 1257 μm . The slot spacing corresponds to a supermode spacing of approximately 430 GHz. The slot width is 1 μm , and the slot depth is equal to the ridge depth (1.75 μm). Vernier tuning between the slotted and gain sections allows single mode lasing to be achieved [17]. The final slot is deep etched to form an etched facet (the deep etch depth is 3 μm).

The master laser then couples into a waveguide which bends around at an angle of 157.5° anticlockwise through a radius of 130 μm . The waveguide is deep etched to increase optical confinement and reduce bend loss, and uses a combination of linear and constant curvature through the bend to further reduce loss. Further details on these bends can be found in [16,18]. The curved waveguide couples through a 7° shallow slot (used for electrical isolation) into a 100 μm linear taper which tapers the waveguide from 2.5 μm to 3.5 μm . The taper couples to the 1x2 MMI which has a length of 116 μm and a width of 10 μm . The two output waveguides from the MMI have a pitch of 5 μm , and taper linearly from 3.5 μm to 2.5 μm over a length of 100 μm , followed by 7° shallow electrical isolation slots. The MMI output arm, which leads to Slave R (right), couples to an identical 157.5° bend described earlier, this time rotating the waveguide clockwise. The MMI output arm which leads to Slave L (left) couples to a short bend which rotates around 22.5° anticlockwise before continuing along a straight waveguide. These 2 coupling arms were designed to have identical lengths, they are both deep etched, and share an electrical contact pad. All features were etched with an Inductively Coupled Plasma (ICP) etcher with etch chemistry $\text{Cl}_2/\text{CH}_4/\text{H}_2$ (Ratio 10:8:4). The device fabrication process used just 4 lithography mask layers, but was not optimised for high-speed, as a high-speed process with low parasitic capacitance top side contacts typically requires significantly more lithography mask layers. However, top side contacts were still added by taking advantage of the deep etch ending in the n-doped contact layers. This enabled high capacitance contacts that could be used up to 5 GHz [15,16].

The slave lasers, Slave L and Slave R, were designed to be a length of 550 μm , although a slight variation existed due to the cleaving of the device. The slave lasers are both Fabry-Pérot lasers defined by a cleaved facet and an etched facet, and feature ground-signal-ground (GSG) contact pads. Simple, short Fabry Pérot lasers were chosen as slave lasers, as they can be made to operate at a higher frequency than the SFP lasers, enabling higher repetition rate combs. In addition, they enable broad tunable locking to the central emission wavelength of the comb as multiple Fabry Pérot modes are available for locking. The etched facet reflectively was estimated as 22% [14]. Deep etched trenches aid in thermally isolating the slave lasers from the rest of the device. A schematic of the device is shown in Fig. 1(a) with sections labelled. A microscope image of the fabricated device is shown in Fig. 1(b).

The geometry of the device and use of curved waveguides placed the slave laser outputs on opposite sides of the chip, which made it simpler to measure both comb outputs simultaneously with lensed optical fibre, while also leading to a compact footprint for the device. No coating was applied to the cleaved facets.

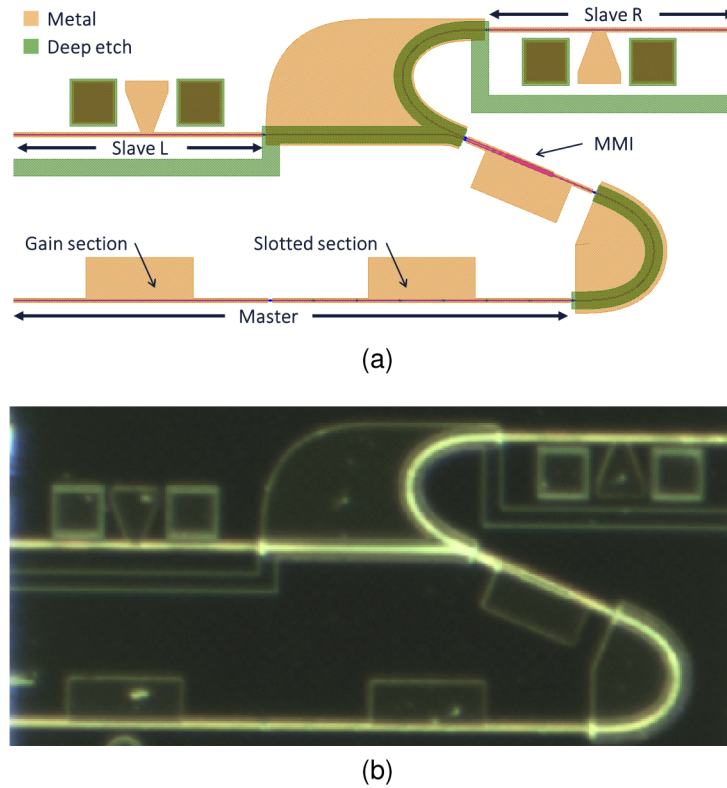


Fig. 1. (a) Schematic of fabricated devices with sections labelled. (b) Microscope image of fabricated devices. The PIC size is $1650\mu\text{m}$ long and $700\mu\text{m}$ wide.

3. Characterisation

The device was mounted on a thermally controlled brass chuck maintained at 20°C . 5 DC (direct current) probe needles were used to make contact with the 2-section master laser, the MMI, and the coupling waveguides, with a ground-signal (GS) probe used for each of the slave lasers. Lensed optical fibre was used to couple light from the slave and master facets.

To start, the slave lasers were characterised individually. The optical output power and voltage was recorded as a function of input current (LI and VI) over a current range of 0-50 mA. These results are shown in Figs. 2(a) and 2(b).

Figure 2(a) shows better electrical contact for Slave L. Contact issues could be due to how the chip is resting on the chuck. From Fig. 2(b) we can estimate the threshold current of the slave lasers to be approximately 25 mA. The spectra of the laser output were also recorded for each of the slave lasers at 50 mA. These are shown in Fig. 3(a), showing typical Fabry-Pérot behaviour. A Fourier analysis of these spectra was used to determine the length of the lasers, which is shown in Fig. 3(b). From this, we can estimate the length of Slave L as $550\mu\text{m}$, and Slave R as $535\mu\text{m}$.

The optical output power and voltage as a function of input current (LIV) was recorded from the master laser, Fig. 4(a), which shows the threshold current to be approximately 40 mA. As the master laser has two sections, both sections were connected to the same current source to perform the LIV. An optical spectrum from the master laser was recorded with the gain section biased at 62 mA, and the mirror section biased at 40 mA. Varying the bias in both sections allows the laser's wavelength to be tuned via the Vernier effect. A discussion on the tunability of slotted Fabry-Pérot lasers is outside the scope of this publication; details can be found in Refs. [17,19].

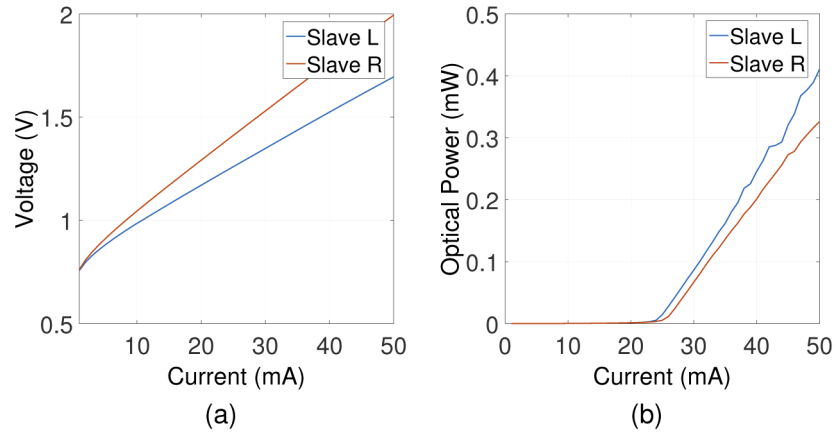


Fig. 2. (a) IVs for both slave lasers. (b) LIs for both slave lasers showing the threshold current of around 25 mA.

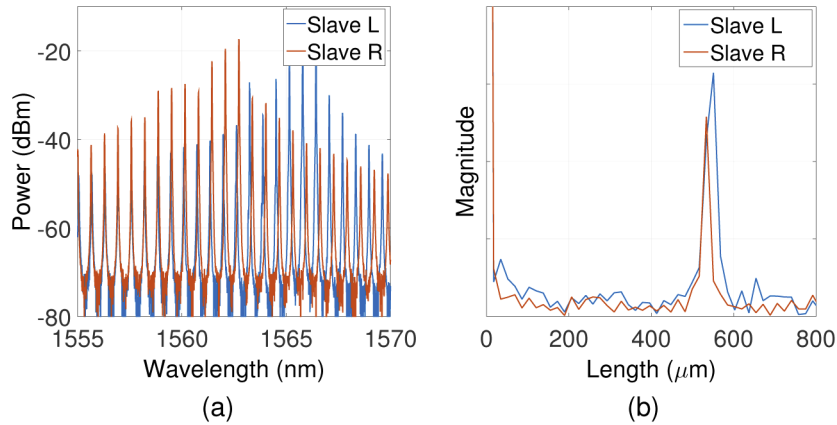


Fig. 3. (a) Emission spectra of the slave lasers biased at 50 mA. (b) Fourier analysis of optical spectra indicating the length of the cavity.

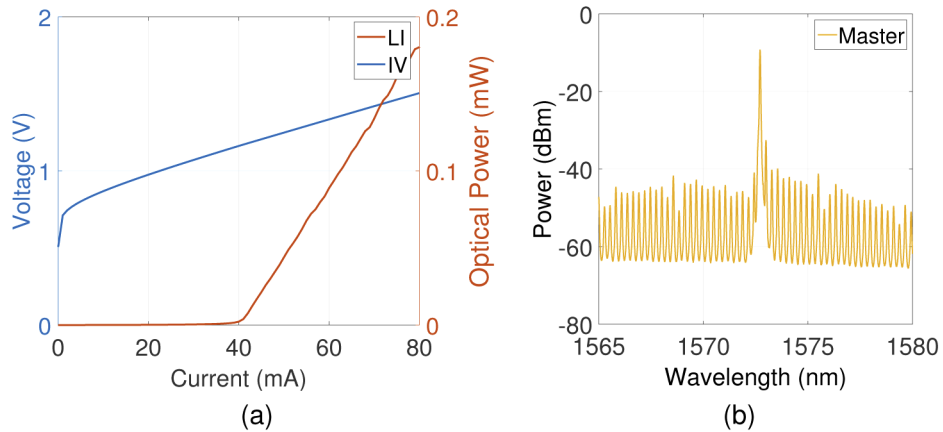


Fig. 4. (a) Master laser LIV. (b) Emission spectrum of the master laser with its gain and mirror sections biased at 75 mA and 60 mA respectively.

To couple the master laser with the slave lasers, the coupling arms and MMI were biased. The MMI was biased at 30 mA, the arm between the master and the MMI was biased at 20 mA, and the arms between the MMI and the slaves were biased at 25 mA (this was 25 mA to share between the arms as they share a contact pad). The master laser was biased at 75 mA and 60 mA for the gain and mirror sections respectively. The slave lasers were biased at 50 mA each. The resulting "single-mode" spectra measured from the slave laser facets is shown in Fig. 5(a). The output measured from the master laser facet is plotted in Fig. 5(b). While it was possible to measure the output from both slave lasers almost simultaneously, one optical fibre had to be coupled to the master laser facet to measure the output. The master laser was biased at approximately 3.4 times threshold which should reduce the perturbing impact of the slave outputs coupled back into the master [20]. At this bias, the master output power is approximately 2 mW. Assuming perfect 50/50 coupling by the MMI, and not accounting for gain/loss in the coupling arms, the injection ratio of the slave lasers can be approximated as 1/2 and 1/1.7 for the left and right slaves respectively. In addition some detuning of the slave lasers was required to optimise the injection locking.

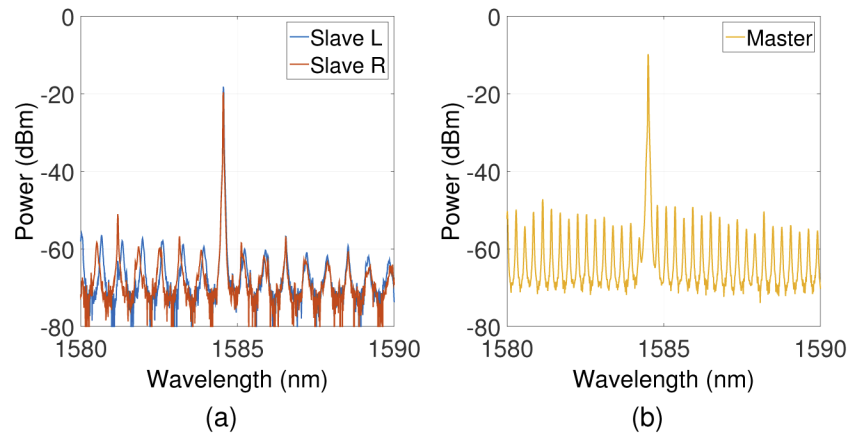


Fig. 5. (a) Optical spectra recorded from the slave lasers biased at 50 mA and injection-locked to the master laser. (b) Master laser spectrum with the master laser biased at 75 mA and 60 mA for the gain and mirror sections respectively.

From Figs. 5(a) and 5(b), it can be seen that both slave lasers are locked to the master laser wavelength of approximately 1584.5 nm.

4. Dual comb generation

Bias tees were used to provide simultaneous DC and RF signals to the slave lasers. An RF signal generator was used to apply a 24 dBm 5 GHz sinusoidal signal to Slave L, and a 24 dBm 4.1 GHz sinusoidal signal to Slave R. These repetition rates were chosen to allow the comb lines to be easily discernible on our optical spectrum analyser. The line spacing can be adjusted directly via the repetition rate of the RF generator. An S_{11} analysis performed using a Vector Network Analyser showed that for a 4.1 GHz and 5 GHz signal, 28% and 26% of the signal is absorbed by the device. This is due to the impedance mismatch between the 50 Ω signal generator and the laser. All DC biases were kept the same as before. The resulting optical combs, as measured from each of the slave facets, are shown in Fig. 6(a). The output from the master laser was then measured and is plotted in Fig. 6(b). Locking both slave lasers to the same master has the unfortunate consequence that the centre wavelength of both combs is locked to the master, which limits the applications using the dual combs.

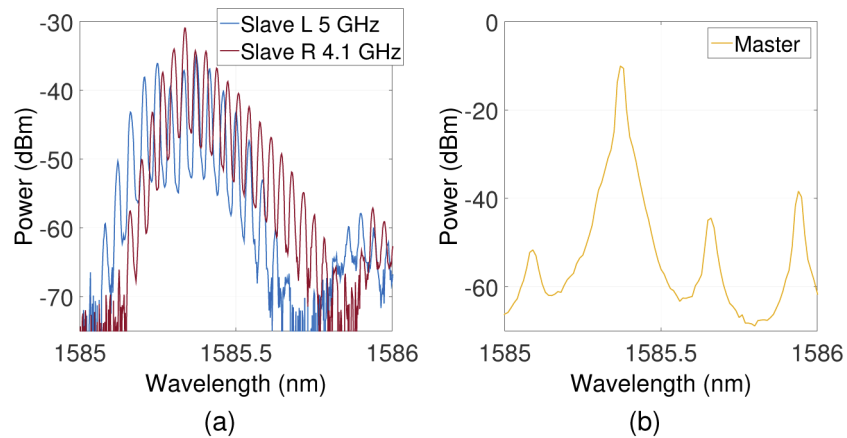


Fig. 6. (a) Dual comb spectra. Slave L is the left slave laser modulated at 5 GHz. Slave R is the right slave laser modulated at 4.1 GHz. (b) Master laser spectrum while the slave lasers are gain-switched.

The lasing wavelength of the master laser is slightly perturbed by the feedback from the slave lasers, but remains single mode. This is in contrast to a previous single comb design outlined in [7], where the master and slave were integrated beside each other. In that case the master laser output was greatly perturbed by feedback from the slave and was indistinguishable from the slave laser output.

Thus by coupling the master laser to the slave laser through the MMI, a greater level of isolation has been achieved for the master laser.

5. Conclusion

In this paper, a single-mode master laser has been monolithically integrated with two high speed Fabry-Pérot slave lasers using a 1x2 multimode interference coupler. The master laser is used to injection lock both slave lasers, which are each gain switched at different frequencies creating two different optical combs. Two different facets are used for the outputs of the slave lasers, thus enabling easier coupling of both lasers into optical fibre. To the best of our knowledge, this is the first demonstration of a monolithically integrated dual optical frequency comb source. 4.1 GHz and 5 GHz combs were generated from Fabry-Pérot slave lasers injection-locked to a common Slotted Fabry-Pérot master laser.

Funding

Enterprise Ireland (CF-2017-0683); Science Foundation Ireland (12/RC/2276, SFI/13/IA/1960); Science Foundation Ireland (14/TIDA/2415).

Disclosures

The authors declare no conflicts of interest.

References

1. P. Delfyett, S. Gee, M.-T. Choi, H. Izadpanah, W. Lee, S. Ozharar, F. Quinlan, and T. Yilmaz, "Optical frequency combs from semiconductor lasers and applications in ultrawideband signal processing and communications," *J. Lightwave Technol.* **24**(7), 2701–2719 (2006).
2. P. Anandarajah, R. Zhou, R. Maher, D. M. Gutierrez Pascual, F. Smyth, V. Vujicic, and L. Barry, "Flexible Optical Comb Source for Super Channel Systems," *Opt. Fiber Commun. Conf. Fiber Opt. Eng. Conf.* 2013 **1**, OTh31.8 (2013).

3. I. Coddington, N. Newbury, and W. Swann, "Dual-comb spectroscopy," *Optica* **3**(4), 414 (2016).
4. I. Coddington, W. Swann, and N. Newbury, "Coherent Multiheterodyne Spectroscopy Using Stabilized Optical Frequency Combs," *Phys. Rev. Lett.* **100**(1), 013902 (2008).
5. S. Chandran, A. A. Ruth, E. P. Martin, J. K. Alexander, F. H. Peters, and P. M. Anandarajah, "Off-Axis Cavity-Enhanced Absorption Spectroscopy of 14NH_3 in Air Using a Gain-Switched Frequency Comb at $1.514\ \mu\text{m}$," *Sensors* **19**(23), 5217 (2019).
6. S. Chandran, S. Mahon, A. A. Ruth, J. Braddell, and M. D. Gutiérrez, "Cavity-enhanced absorption detection of H_2S in the near-infrared using a gain-switched frequency comb laser," *Appl. Phys. B* **124**(4), 63 (2018).
7. J. K. Alexander, P. E. Morrissey, L. Caro, M. Dernaika, N. P. Kelly, and F. H. Peters, "On-Chip Investigation of Phase Noise in Monolithically Integrated Gain-Switched Lasers," *IEEE Photonics Technol. Lett.* **29**(9), 731–734 (2017).
8. P. M. Anandarajah, R. Maher, Y. Q. Xu, S. Latkowski, J. O'Carroll, S. G. Murdoch, R. Phelan, J. O'Gorman, and L. P. Barry, "Generation of coherent multicarrier signals by gain switching of discrete mode lasers," *IEEE Photonics J.* **3**(1), 112–122 (2011).
9. R. Zhou, P. M. Anandarajah, D. G. Pascual, J. O Carroll, R. Phelan, B. Kelly, and L. P. Barry, "Monolithically Integrated 2-Section Lasers for Injection Locked Gain Switched Comb Generation," *Opt. Fiber Commun. Conf. Fiber Opt. Eng. Conf.* 2013 **1**, 1–3 (2014).
10. J. K. Alexander, P. E. Morrissey, H. Yang, M. Yang, P. J. Marraccini, B. Corbett, and F. H. Peters, "Monolithically integrated low linewidth comb source using gain switched slotted Fabry-Perot lasers," *Opt. Express* **24**(8), 7960–7965 (2016).
11. B. Jerez, P. Martín-Mateos, E. Prior, C. de Dios, and P. Acedo, "Gain-switching injection-locked dual optical frequency combs: characterization and optimization," *Opt. Lett.* **41**(18), 4293–4296 (2016).
12. A. Dutt, C. Joshi, X. Ji, J. Cardenas, Y. Okawachi, K. Luke, A. L. Gaeta, and M. Lipson, "On-chip dual-comb source for spectroscopy," *Sci. Adv.* **4**(3), e1701858 (2018).
13. P. E. Morrissey, N. Kelly, M. Dernaika, L. Caro, H. Yang, and F. H. Peters, "Coupled Cavity Single-Mode Laser Based on Regrowth-Free Integrated MMI Reflectors," *IEEE Photonics Technol. Lett.* **28**(12), 1313–1316 (2016).
14. J. K. Alexander, P. E. Morrissey, L. Caro, M. Dernaika, N. P. Kelly, and F. H. Peters, "Integratable Optical Comb Source for Coherent Communications Systems," in *Conference on Lasers and Electro-Optics*, (OSA, Washington, D.C., 2017), p. SW10.3.
15. L. Caro, N. P. Kelly, M. Dernaika, M. Shayesteh, P. E. Morrissey, J. K. Alexander, and F. H. Peters, "A facetless regrowth-free single mode laser based on MMI couplers," *Opt. Laser Technol.* **94**, 159–164 (2017).
16. M. Dernaika, N. P. Kelly, L. Caro, and F. H. Peters, "Single mode semiconductor laser based on coupled cavities of an active ring laser and Fabry Perot," *IET Optoelectron.* **12**(3), 118–121 (2018).
17. D. Byrne, J. Engelstaedter, W.-H. Guo, Q. Yin Lu, B. Corbett, B. Roycroft, J. O'Callaghan, F. Peters, and J. Donegan, "Discretely Tunable Semiconductor Lasers Suitable for Photonic Integration," *IEEE J. Sel. Top. Quantum Electron.* **15**(3), 482–487 (2009).
18. R. N. Sheehan, S. Horne, and F. H. Peters, "The design of low-loss curved waveguides," *Opt. Quantum Electron.* **40**(14–15), 1211–1218 (2008).
19. D. Byrne, Q. Lu, W. H. Guo, J. F. Donegan, B. Corbett, B. Roycroft, P. Lambkin, J. P. Engelstaedter, and F. Peters, "A facetless laser suitable for monolithic integration," in *2008 Conference on Quantum Electronics and Laser Science Conference on Lasers and Electro-Optics, CLEO/QELS* pp. 2008–2010 (2008).
20. P. E. Morrissey, W. Cotter, D. Goulding, B. Kelleher, S. Osborne, H. Yang, J. O'Callaghan, B. Roycroft, B. Corbett, and F. H. Peters, "On-chip optical phase locking of single growth monolithically integrated slotted fabry perot lasers," *Opt. Express* **21**(14), 17315 (2013).